Astron. Astrophys. 345, 905–914 (1999)

ASTRONOMY AND ASTROPHYSICS

The peculiar post–AGB supergiant IRAS 04296+3429: optical spectroscopy and its spectral energy distribution

V.G. Klochkova[1], **R. Szczerba**[2], **V.E. Panchuk**[1], **and K. Volk**[3]

[1] Special Astrophysical Observatory, N.Arkhyz, 357147 Russia
[2] N. Copernicus Astronomical Center, PL-87-100 Toruń, Poland
[3] The University of Calgary, Calgary, Alberta T2N 1N4, Canada

Received 8 April 1998 / Accepted 5 March 1999

Abstract. The optical spectrum of the infrared source IRAS 04296+3429 (optical counterpart – G0 Ia star, V = 14.2) was obtained with the echelle spectrometer PFES at the prime focus of the 6 m telescope. We discover *emission* bands (0,0) and (0,1) of the Swan system of the C_2 molecule in the optical spectrum of IRAS 04296+3429. Comparison with the spectrum of the Hale-Bopp comet leads us to propose that in both cases the same mechanism (resonance fluorescence) is responsible for the emission in the C_2 molecular bands.

Several strong absorption features whose positions coincide with known diffuse interstellar bands (DIBs) are revealed in the spectrum of IRAS 04296+3429.

The infrared spectrum of IRAS 04296+3429 shows the famous 21 μm feature (Kwok et al. 1989), but this object has not been observed by KAO (Omont et al. 1995). However, like IRAS 05113+1347, IRAS 05341+0852 and IRAS 22223+4327 (Kwok et al. 1995, Szczerba et al. 1996), our detailed modelling of its spectral energy distribution suggested that this source also should show the 30 μm band. In fact, *ISO* discovered a broad, relatively strong feature around 30 μm for IRAS 04296+3429 (Szczerba et al. 1999).

The surface chemical composition of the source IRAS 04296+3429 is metal-deficient (the averaged value of the abundances of the iron group elements Ti, V, Cr and Fe relative to the solar values is $[\mathrm{M/H}]_\odot = -0.9$) and has been considerably altered during the evolution: carbon, nitrogen and s-process elements are overabundant relative to the metallicity.

The totality of physical and chemical parameters derived for IRAS 04296+3429 confirms a relation between presence of the feature at 21 μm in the spectrum of a carbon rich star and an excess of the s-process elements.

Key words: stars: abundances – stars: AGB and post-AGB – stars: individual: IRAS 04296+3429

1. Introduction

This paper is a continuation of our series of papers on the investigation of stars which are believed to be in the post–Asymptotic Giant Branch (post–AGB) stage of evolution (Klochkova 1995; Začs et al. 1995, 1996; Klochkova & Panchuk 1996a, 1998; Klochkova et al. 1997a; Klochkova & Mishenina 1998). The post–AGB stars (hereafter also referred to as proto–planetary nebulae – PPNe) being in the transition phase from AGB to planetary nebulae offer an opportunity to study in detail a chemical composition which has undergone changes due to nucleosynthesis and mixing processes in the course of the stars evolution. Here we present new results for the peculiar supergiant with a large infrared excess IRAS 04296+3429.

On the 12/25/60 μm colour–colour diagram from the IRAS data infrared source IRAS 04296+3429 (hereafter IRAS 04296), associated with a faint carbon–rich star (Omont et al. 1993; Loup et al. 1993) classified as type G0 Ia by Hrivnak et al. (1994), is located in the region occupied by planetary nebulae, non–variable OH/IR stars, and proto–planetary nebulae (Iyengar & Parthasarathy 1997). The object IRAS 04296 belongs to the small group of sources which show a spectral feature around 21 μm (Kwok et al. 1989). This feature is seen only for some post–AGB objects and has not been detected either in the preceding (AGB) nor in the succeeding (PN) evolution stage. Note that a search for new 21 μm emitters by means of *ISO SWS* observations among candidates selected by Henning et al. (1996) failed to give any detections (Henning, private communication). Using a medium-resolution (3 Å) optical spectrum, Hrivnak (1995) found that IRAS 04296 is a strongly reddenned (E(B-V) = 1.3) G-star with features indicative of high luminosity, with molecular absorption features of C_2 and rarely observed features of C_3 *of circumstellar origin* and quite strong absorption lines of s-process elements (Ba, Sr, Y) indicating that outer layers of the atmosphere of IRAS 04296 have been enriched by products of nucleosynthesis. Therefore this star is very well suited for the study of detailed chemical abundances which have been changed by the third dredge–up. Indeed, Decin et al. (1998), using high resolution spectra, obtained the chemical abundance pattern for this object and concluded that its metal–deficient, carbon–rich atmosphere has large overabundances of s–process elements.

In Sect. 2 we describe our observational material for IRAS 04296 and discuss its molecular features, comparing them with the corresponding spectrum of the Hale–Bopp comet.

Send offprint requests to: V.G. Klochkova (valenta@sao.ru)

Sect. 3 is devoted to presentation of the main parameters and detailed analysis of the chemical composition of IRAS 04296 derived from our optical spectra. The next section presents modelling of spectral energy distribution for this source with the aim to get insight into its physical parameters (mainly to determine the stellar effective temperature which is crucial for the chemical composition estimation). Finally, in Sect. 5 we discuss the results obtained and compare them to the results for related objects.

2. Optical spectrum of IRAS 04296

2.1. Observations and spectra reduction

We have obtained spectra of IRAS 04296 with the CCD (1140×1170 pixels) equipped echelle spectrometer PFES mounted at the prime focus of the 6 m telescope of SAO RAS (Panchuk et al. 1998). The echelle-grating with $75\,\mathrm{gr/mm}$ and with a blaze angle of $\Theta = 64.3^{\circ}$ was used. A diffraction grating with $300\,\mathrm{gr/mm}$ was used as the cross-disperser. The camera has f = 140 mm. The projected angular size of the input slit is 0.54 arc sec.

We observed IRAS 04296 on October 07, 1996 (JD2450363.6) and February 26, 1997 (JD2450506.3). The echelle frames with 25 echelle-orders cover the spectral region $\lambda\lambda$ 4420–8300 Å. The average spectral resolution was 0.4 Å. The signal-to-noise ratio was in the range 50–110 for different spectral orders.

All usual procedures needed for echelle-images reduction (bias subtraction, cosmic ray removal, optimal order extraction, rebinning) were made using the ECHELLE context of the MIDAS system. A Gaussian function approximation was made for the measurement of equivalent widths. The comparison spectrum source was an argon-filled thorium hollow-cathode lamp.

The distinctive features of the optical spectrum of the source IRAS 04296 are a peculiar profile of the H_α line (see Fig. 1), molecular emission bands and very strong absorption lines of ionized atoms of s–process elements (Y, Zr, Ba, La, Ce, Pr, Nd). For example, the equivalent widths of Ba II lines (6141 and 6496 Å) exceed 0.6 Å.

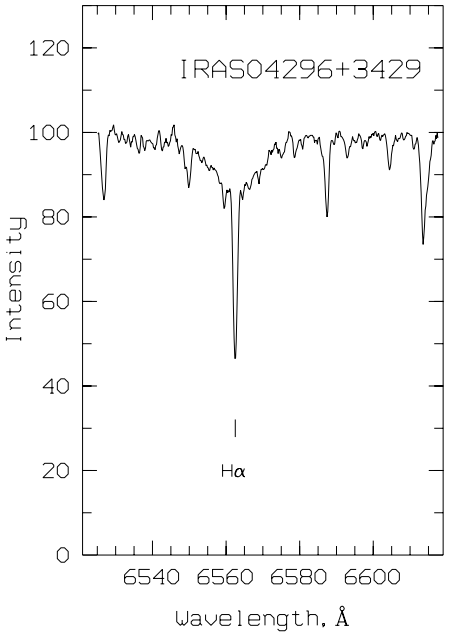

Fig. 1. The IRAS 04296+3429 spectrum near H_α.

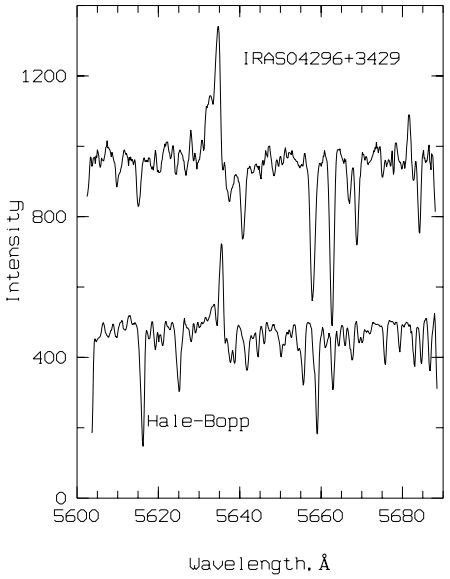

Fig. 2. Comparison of the IRAS 04296 + 3429 C_2 Swan band head (0;1) at λ = 5635 Å with that for the Hale-Bopp comet nuclei

2.2. Emission molecular bands

Absorptional bands of several molecules (C_2, CN, TiO, etc.) are often present in the spectra of post-AGB stars (see, for example, Hrivnak 1995; Bakker et al. 1997). However, molecular *emission* features are only very rarely observed in the optical spectra of PPNe. One such example is RAFGL 2688 (the Egg Nebula) for which Crampton et al. (1975) observed emission features of the C_2 molecule in a medium resolution spectrum. On the other hand, it is well known that cometary nuclei spectra show prominent Swan band emission.

In both spectra of IRAS 04296 we have discovered strong *emission* in the (0;0) and (0;1) bands of the Swan system of the C_2 molecule. On Figs. 2–4 we present a comparison between the spectrum of IRAS 04296 (observed on February, 26, 1997) and that of the Hale-Bopp comet (observed on March 30, 1997 with the same spectrometer) around bands (0;1), (0;0) and (1;0), respectively. From Figs. 2–4 it is clear that emission band (1;0) at 4735 Å is absent in the spectrum of IRAS 04296 while the bands (0;1) at 5635 Å and (0;0) at 5165 Å are reliably measured. Hrivnak (1995) obtained the spectrum of IRAS 04296 inside the blue spectral region, 3872–4870 ÅÅ, therefore he could not observe emission features of C_2 at 5165 and 5635 ÅÅ.

To understand the observed ratios between different bands, we have estimated the temperature function for monochromatic coefficient of absorption per molecule (σ_λ) for the Swan bands in the "just overlapping" approximation (JOA, Golden 1967). For the microturbulent velocity $\xi_t = 7\,\mathrm{km/sec}$ this approxima-

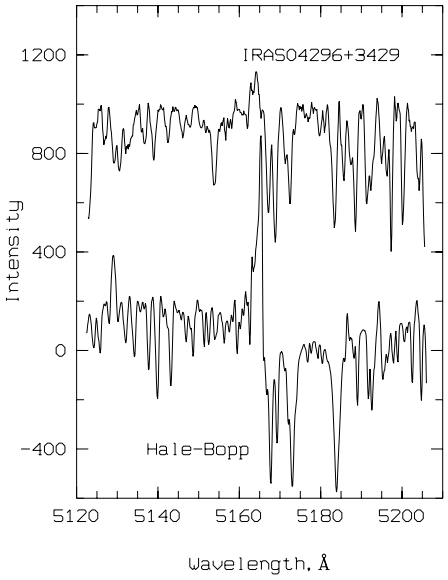

Fig. 3. The same as Fig. 2 but for C_2 Swan band head (0;0) at λ = 5165 Å

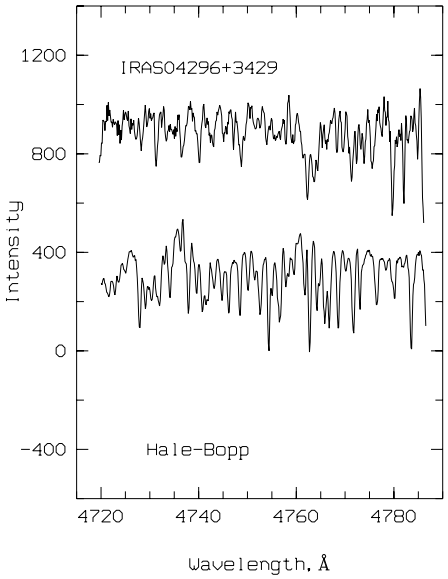

Fig. 4. The same as Fig. 2 but for C_2 Swan band head (1;0) at λ = 4735 Å

tion works well near the band heads. Values of σ_λ for band heads of (0;0) at 5165 Å and (1;0) at 4735 Å coincide within 0.2 dex for the temperatures range 3000–7000 K, while σ_λ for the band (0;1) at 5635 Å is systemically lower by about 0.6 dex. Taking into account these relations between σ_λ's for different band heads and since we do not observe the 4735 Å band in RAFGL 2688 and IRAS 04296, we can conclude that it is impossible to describe the intensity ratios of C_2 emission bands for these objects by means of an equilibrium vibrational temperature in the 3000–7000 K range.

To explain emission bands intensities for comets the mechanism of resonance fluorescence has been proposed (Zanstra 1928, Swings 1941). In that case population of vibration–rotational levels for the molecule is described by the Boltzmann approximation, however the value of *T* in the exponent no longer has the meaning of equilibrium temperature but it is a distribution parameter only. We suggest that the same mechanism could be responsible for the observed emission bands of IRAS 04296. However, it is clear from Figs. 2–4 that there are significant differences in the equivalent widths of the emission bands in the spectra of our supergiant and of the Hale–Bopp comet nucleus. They could be explained by a difference of radiation fluxes which illuminate C_2 molecules in these objects. The temperature of IRAS 04296 ($T_{\rm eff}$ around 6300 K) is sufficiently higher than that for the Sun, therefore the band (1,0) at 4735 Å for IRAS 04296 should be stronger than that for the Hale-Bopp comet nuclei. However, Fig. 4 shows the opposite behaviour. This could mean that the radiation field of IRAS 04296 which excites the C_2 molecules is strongly reddened by matter located between its photosphere and the region which produces the C_2 emission.

Together with the emission bands of the Swan system (Klochkova et al. 1997b) absorption bands of the Phillips system (1:0), (2;0), (3;0) have been revealed in the spectrum of IRAS 04296 (Bakker et al. 1997). Let us try to explain this phenomenon within the resonance fluorescence mechanism ordinary used to interpret comets' spectra. As a first approximation, we assume that the vibrational distribution corresponds to the effective temperature of the star illuminating a circumstellar envelope if vibrational transitions in the low triplet state of a homonuclear molecule are strictly forbidden. But even when interpreting comets' spectra such an approach appears to be too poor. The intensity distributions for different systems of bands and for bands of individual systems of the resonance fluorescence of the C_2 molecule have been considered in papers by Krishna Swamy & O'Dell (1977, 1979, 1981). The intensities of bands have been calculated taking into account the excitation of the Swan, Ballick-Ramsay and Fox-Herzberg triplet systems, Phillips and Milliken singlet systems as well as singlet-triplet transitions in low states. It has been shown, in particular, that at the value of the moment of singlet-triplet transitions $|R_e|^2 = 10^{-5}$ and at the heliocentric distance of a comet d=1 a.u. the ratios of intensities of sequences $\Delta\nu = 0,\ 1,\ -1$ in the Phillips system to the intensity of sequence $\Delta\nu = 0$ of the Swan system is equal to 0.094, 0.11 and 0.04, correspondingly (Krishna Swamy & O'Dell 1981). This agrees well with results of measurement of comets' spectra. Using these results of Krishna Swamy & O'Dell (1981), we may suppose that the intensity of main bands of the Swan system is ten times higher than that in the Phillips system.

Now consider the case of IRAS 04296. Let us add such an emission spectrum of the C_2 on the stellar continuum. In order to observe the emission bands of both the Swan and the Phillips systems over the continuum in such a combined spectrum, the stellar flux at λ = 5165 Å must be at least 10 times higher than near λ = 7720 Å. From Kurucz's (1979) tables it follows that the ratio of the fluxes near these wavelengths for the Sun (the emitter in the case of comets) is equal to $F_{\lambda 5175}/F_{\lambda 7750} = 1.5$. For the model with $T_{\rm eff}$ = 6300 K this

ratio is equal to $F_{\lambda5175}/F_{\lambda7750} = 1.9$. From the real spectral energy distribution observed for IRAS 04296 (Kwok 1993) the ratio of the fluxes is essentially smaller: $F_{\lambda5165}/F_{\lambda7720} = 0.1$. Therefore, the conditions to observe the absorption bands of the Phillips system and the emission bands of the Swan system may arise inside the circumstellar envelope of IRAS 04296.

2.3. Radial velocity of the IRAS 04296

We measured the radial velocity V_r using our best spectrum, that obtained in February, 1997. The average value of the radial velocity from numerous metal lines ($V_r = -56.0 \pm 0.8\,km/s$) and from the H_α absorption line ($V_r = -54.5\,km/s$) agrees within the accuracy of measurement. This radial velocity is consistent with a membership of an old population as suggested by the low metallicity (see Table 1). It should be noted also that the value of radial velocity we derived agrees with the value of $V_r = -59\,km/s$ which was given by Omont et al. (1993) from CO data and $V_r = -62\,km/s \pm 1.0\,km/s$ by Decin et al. (1998) from optical spectrum. There is still no sign of an essential temporal variability of V_r for the object.

2.4. Absorption bands identified with DIBs

From comparison of observed and synthetic spectra of IRAS 04296 we discovered some strong absorptional features whose positions coincide with known diffuse interstellar bands (DIBs) (Jenniskens et al. 1994). In Fig. 5 we illustrate the presence of DIB's by showing a spectral region of IRAS 04296. We have calculated the synthetic spectrum using the code STARSP (Tsymbal 1995) and the atmospheric parameters and abundances of chemical elements we here obtained. It should be noted that for such a comparison in the spectral range near λ 6270–6310 Å the telluric spectrum has been removed from the observed spectrum.

In the following paper we plan to study in detail such identified with DIB's absorptions, we have revealed in the spectra of several related objects (IRAS 04296, IRAS 23304+6147, IRAS222223+4327), here we limited ourself by such short information.

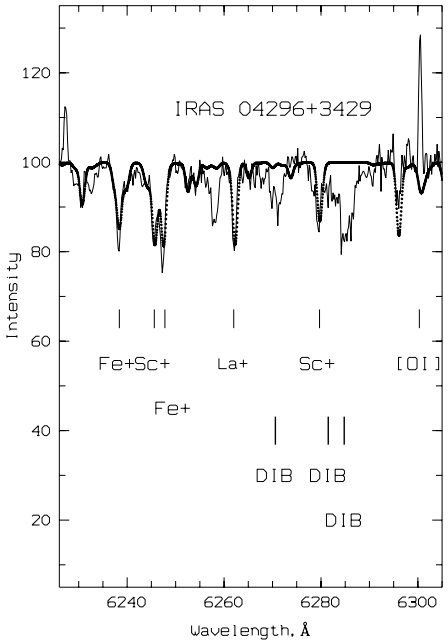

Fig. 5. The observed (line) and synthetic (dots) spectra of the object IRAS 04296 + 3429 near absorbtional features identified with the DIBs. The telliric spectrum was removed from the observed spectrum of the object

3. Determination of atmospheric parameters and calculation of chemical composition

For the understanding of an object at an advanced evolutionary stage, it is very important to know its metallicity and detailed chemical abundance pattern. Our echelle spectra provide such a possibility due to their large wavelengths coverage.

To study the chemical composition, we have used the plane-parallel homogeneous models generated by the MARCS program (Gustafsson et al. 1975). It should be noted, however, that unstable and very extended atmospheres of supergiants probably require more advanced model atmospheres. Therefore, our results should be treated as only preliminary ones. For a chemical composition calculation by the model atmosphere method, one needs to know the values of the effective temperature (T_{eff}), surface gravity (log g) and microturbulent velocity (ξ_t). Determination of T_{eff} is problematic even for normal supergiants due to their extended atmospheres and significant non-LTE effects. In the case of so peculiar a supergiant as IRAS 04296, for which the energy distribution is strongly distorted by interstellar and circumstellar extinction, the determination of T_{eff} is the most difficult problem. We cannot use for this purpose equivalent widths and profiles of H I lines (well known criteria of atmospheric conditions for normal supergiants), since these lines are strongly distorted in the spectrum of IRAS 04296 as seen in Fig. 1.

Therefore, we have applied the spectroscopic method for temperature determination of IRAS 04296, forcing the abundance derived for each line to be independent of the lower excitation potential (EP). We have estimated that T_{eff} = 6300 K with an internal uncertainty ΔT_{eff} = 250 K. To check the reliability of our determination we have modelled the spectral energy distribution for this source (see Sect. 4) and got a very similar temperature near 6500 K. The surface gravity log g = 0.0 was estimated through the ionization balance of the Fe I and Fe II abundances. The errors on the parameter log g is determined by forcing a maximum difference between ϵ (Fe I) and ϵ (Fe II) to be 0.1 dex (where here and hereafter, $\log\epsilon(X) = \log N(X) - \log N(H)$). It should be noted that the hydrogen abundance $\log N(H) = 12$. Such a difference is achieved by varying the log g value by ±0.2 keeping other parameters (T_{eff} and ξ_t) constant. The microturbulent velocity value based on equivalent widths (W) of Fe I and Fe II lines is quite high, equal to 7 km/s. This value is determined with an uncertainty of $\pm1.0\,km/s$, which is typical for F, G–supergiants.

To illustrate the choice of model parameters for the object IRAS 04296 in the Fig. 6 are shown the excitation potential – abundance diagram and the equivalent width – abundance diagram for lines of neutral (dots) and ionized (crosses) iron atoms. As follows from this figure, there are no essential dependences for values considered. The large dispersion is mainly explained by errors of measurement of equivalent widths of weak absorption lines for such a faint object as the IRAS 04296 (see, for example, the similar dispersion on the Fig. 1 in the paper by Decin et al. (1998) for the brighter object IRAS 22223+4327, V=9.7).

We have checked the determination of IRAS 04296 model parameters using weaker FeI and FeII lines and concluded that the parameters are steady within the erorr box up to W = 100–150 mÅ. This can also be seen from Fig. 6.

It is well known that the plane-parallel static model atmosphere method does not give correct abundances for high luminosity stars (luminosity classes Ia, Ia+). The profiles of the spectral lines observed are broadened by non-thermal mechanisms whose influence may be variable at different levels in the atmosphere. Therefore, to obtain more reliable estimates of chemical element abundances we use weak lines with W <250 mÅ. The average values of the equivalent widths $\overline{\mathrm{W}}$ we used for the abundances calculations are also given in Table 1. Only the BaII abundance was calculated using 3 very strong lines: W(λ 5853.67) = 464 mÅ, W(λ 6141.71) = 679 mÅ and W(λ 6496.90) = 738 mÅ, because the weaker lines of this element were not available. In general, the weak lines formed in deeper atmospheric layers are more correctly described by the standard static model. The limitation of equivalent width of lines used to W <250 mÅ significantly reduces the influence of uncertainty in the choice of ξ_{t}. Note, however, that the main factor in the abundance errors for most species remains the uncertainty of the $\mathrm{T_{eff}}$ value. Therefore, we have checked our estimation of $\mathrm{T_{eff}}$ by modelling of spectral energy distribution for IRAS 04296.

Computed abundances of 26 chemical elements are presented in Table 1. In the head of the Table 1 parameters of the adopted model atmosphere are shown. The dependence of chemical composition determination on uncertainties of the model atmosphere parameters is discussed in Začs et al. (1995). In the second column of Table 1 derived abundances are given as $\log\epsilon\,(\mathrm{X})$, while in the third column estimated uncertainties of $\sigma = \Delta\log\epsilon\,(\mathrm{X})$ are shown. In the next column, the number of spectral lines used for chemical composition calculation is indicated.

A lot of absorption lines of different elements (CNO-elements, light metals, iron group elements, Ce, Nd, Eu) have been reliably measured in the spectrum of IRAS 04296. It is important that we have not found any dependence of the abundances of these species on the equivalent width or on the excitation potential. Therefore the microturbulent velocity does not vary between different chemical elements.

The gf–values for most of the spectral lines used for the abundance calculations were taken from the list used by Luck (1991). The S and CNO-abundances were determined by using the gf–data from Waelkens et al. (1991) and Giridhar et al. (1994). The list of lines with the adopted gf–values, excitation potentials of the lower level and equivalent widths we measured for the object IRAS 04296 are available by e-mail (valenta@alba.sao.ru).

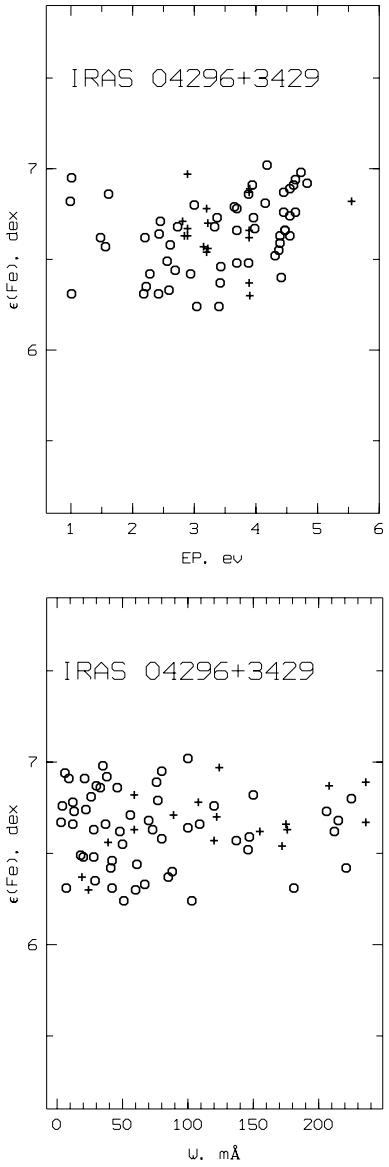

Fig. 6. *Upper:* iron abundance FeI (circles) and FeII (crosses) calculated for IRAS 04296 with model parameters $\mathrm{T_{eff}} = 6300\,\mathrm{K}$, $\log\mathrm{g} = 0.0$ and $\xi_{\mathrm{t}} = 7.0\,\mathrm{km/sec}$ using lines with different EP of a low level; *bottom:* the same as a function of the equivalent width W

To verify the method of analysis we observed with the same spectral device the normal supergiant α Per. The same procedures for processing and the same list of lines were used for analysis of the α Per spectrum. This supergiant, whose parameters, $\mathrm{T_{eff}} = 6500\,\mathrm{K}$, $\log\mathrm{g} = 1.2$, $\xi_{\mathrm{t}} = 4.7\,\mathrm{km/sec}$ are very close to the object studied, is very convenient as a standard for the method testing because of its membership in the young open cluster $\alpha\mathrm{Per}$ which has solar chemical composition (Klochkova & Panchuk 1985; Boesgaard 1989). Using its membership of this cluster, we may predict that $\alpha\,\mathrm{Per}$ also has normal solar

Table 1. Model atmosphere parameters adopted and abundances of chemical elements. Here, n is number of lines used for calculation, σ – the standard deviation, $\overline{\mathrm{W}}$ – the average equivalent width, in $\mathrm{m\AA}$, of lines used for the content calculation

	IRAS 04296+3429				α Per			
	$T_{\rm eff}$ = 6300 K, log g = 0.0, ξ_t = 7.0 km/s				$T_{\rm eff}$ = 6500 K, log g = 1.2,ξ_t = 4.7 km/s			
Element	$\log\epsilon(\mathrm{X})$	σ	n	$\overline{\mathrm{W}}$	$\log\epsilon(\mathrm{X})$	σ	n	$\overline{\mathrm{W}}$
Li I	≥ 2.70		1	32				
C I	8.55	0.46	21	69	8.16	0.14	13	47
N I	7.96	0.10	4	99	8.35	0.10	4	127
O I	8.22	0.05	3	26	8.35	0.06	4	23
Na I	5.91	0.24	3	68	6.48	0.06	4	48
Mg I					7.83	0.03	2	56
Mg II	8.08	0.03	2	254				
Al I	6.66	0.14	3	68	6.57	0.16	4	32
Si I	7.29	0.20	11	37	7.68	0.16	16	45
Si II	6.97		1	22	7.81		1	278
S I	6.80	0.21	7	30	7.53	0.23	2	187
Ca I	5.71	0.30	19	98	6.41	0.22	14	122
Sc II	2.51	0.28	10	164	2.72	0.07	6	119
Ti II	3.91	0.33	5	184	4.78	0.08	4	47
V II	3.26	0.28	4	26	3.54	0.10	4	22
Cr II	4.94	0.28	10	108	5.54	0.12	9	136
Mn I					5.25	0.09	3	63
Fe I	6.66	0.30	55	75	7.48	0.21	111	59
Fe II	6.65	0.22	19	131	7.51	0.09	10	154
Cu I	3.61		1	38	4.66		1	36
Zn I	3.84		1	9				
Y II	2.60	0.14	2	168	2.20	0.40	2	32
Zr I					3.38	0.10	4	6
Zr II	2.38		1	165				
Ba II	3.78	0.47	3	627	2.06		1	212
La II	1.55	0.44	6	116	1.04	0.08	4	20
Ce II	1.53	0.16	5	83				
Pr II	0.61		1	19				
Nd II	1.73	0.31	12	102	0.84	0.08	4	8
Eu II	0.01	0.04	2	20	0.44	0.09	3	20

chemical composition (aside from the expected nonsolar CNO triad abundances relative to iron). As it is shown in Table 1 αPer has indeed the abundances of chemical elements close to solar ones, except for CNO and several elements whose abundances are calculated with a large uncertainity due to a small number of spectral lines used.

4. Spectral energy distribution

Details of the computer code used for solution of the radiative transfer in dusty envelopes can be found in Szczerba et al. (1997). In brief: the frequency–dependent radiative transfer equation is solved for a dust under assumption of spherically–symmetric geometry for its distribution taking into account particle size distribution and quantum heating effects for the very small dust particles.

The modelled source is certainly C–rich (see Omont et al. 1995). Therefore, for modelling of its spectral energy distribution (SED) we assumed that dust is composed of: policyclic aromatic hydrocarbons (PAH) for dust sizes a between 5 and 10 Å (see Szczerba et al. (1997) for details concerning PAH properties), amorphous carbon grains (of AC type from Rouleau & Martin 1991) for $a > 50$ Å, and dust with an opacity obtained from averaging of the absorption efficiences for PAH and AC grains according to the formula:

$$Q_{\mathrm{abs},\,\nu} = \mathrm{f}\,\cdot\,Q^{\mathrm{PAH}}_{\mathrm{abs},\,\nu}(a)\,+\,(1-\mathrm{f})\,\cdot\,Q^{\mathrm{AC}}_{\mathrm{abs},\,\nu}(a),$$

for grain sizes between 10 and 50 Å. Here: f = 1 for a = 10 Å and f = 0 for a = 50 Å. Dust with opacity values constructed in this way allow us to use a continuous distribution of dust grain sizes and fill the gap between properties of carbon–bearing molecules and small carbon grains.

The 21 μm feature was approximated by a gaussian with parameters determined from modelling of IRAS 07134+1005 (centre wavelength equal to 20.6 μm, and width of 1.5 μm) which has the strongest feature among the known 21 μm sources. In the case of 30 μm band we used the addition of two half–gaussians with the same strength and different widths. Initial fit was done to IRAS 22272+5435 and its parameters were: width for short wavelength side $\sigma_{\rm L} = 4\,\mu$m, width for long wavelength side $\sigma_{\rm R} = 9\,\mu$m and central wavelength 27.2 μm (see Szczerba et al. 1997). For modelling of IRAS 04296 we

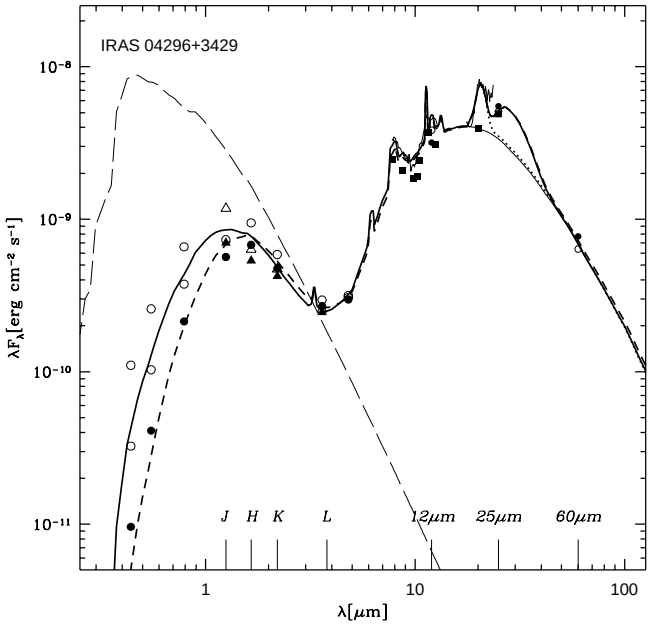

Fig. 7. Fit to the spectral energy distribution of IRAS 04296 + 3429 obtained with empirical opacity function, taking into account quantum heating effects (heavy solid line) and assuming that star radiates according to a model stellar atmosphere calculation for log g = 0.5 and $T_{\rm eff}$ = 6500 K (thin long–dashed line). The heavy dashed line shows the fit obtained for star with $T_{\rm eff}$ = 6000 K. The thin solid line underlying 21 and 30 μm features represents the estimated continuum level

Table 2. Model parameters for IRAS 04296+3429. Precise meaning of the symbols used can be found in Szczerba et al. (1997)

parameter	value
$T_{\rm eff}$	6500 K
log ($L_{\rm star}$ [$L_\odot$])	3.92
d	5.4 kpc
$R_{\rm out}$	0.5 pc
$V_{\rm exp}$	12 km s^{-1}
$R_{\rm in}$(hot dust shell)	6.4 10^{-4} pc
$\overline{T}_{\rm d}$[$R_{\rm in}$(hot dust shell)]	870 K
$\rho_{\rm gas}$ (hot dust shell)	$\sim r^{-2.0}$
$\dot{M}_{\rm post-AGB}$	4.0 10^{-7} $M_\odot$ yr^{-1}
$R_{\rm in}$(main shell)	7.06 10^{-3} pc
$\overline{T}_{\rm d}$[$R_{\rm in}$(main shell)]	270 K
$\rho_{\rm gas}$ (main shell)	$\sim r^{-2.6}$
$\dot{M}^{\rm min}_{\rm AGB}$	1.70 10^{-5} $M_\odot$ yr^{-1}
$\dot{M}^{\rm max}_{\rm AGB}$	2.19 10^{-4} $M_\odot$ yr^{-1}
a_-	5Å
a_+	0.25 μm
p	3.5
$t_{\rm dyn}$	575 yr
$M_{\rm dust}$	0.0071 $M_\odot$

have reduced the strength of this feature by 50%. Superposition of the 21 and 30 μm features was added to the absorption properties of amorphous carbon in order to construct an empirical opacity function (EOF).

In Fig. 7 the best fit obtained from the solution of the radiative transfer problem including quantum heating effects for the PAH grains is shown together with observational data which will be described in detail elsewhere. Note, however, that we present also two sets of photometry (from B to M band) corrected for interstellar extinction (open symbols) according to the average extinction law of Cardelli et al. (1989), assuming that total extinction at V is 1.0 or 2.0 magnitudes and plotting only the smallest and largest value of corrected fluxes at given band. This estimate of the total extinction range can be inferred from the analysis of data presented by Burstein & Heiles (1982).

The best fit to the spectral energy distribution of IRAS 04296 is shown by heavy solid line (see Table 2 for details concerning parameters of the model). Our modelling procedure was such that we tried to get fits to the SED which fall in between the extinction corrected fluxes. In this way, we have taken into account not only the effect of the circumstellar extinction but also of interstellar extinction. The thin long–dashed line represents the input energy distribution of the central star for log g = 0.5 and $T_{\rm eff}$ = 6500 K according to model atmosphere calculations of Kurucz (private communication). The heavy short–dashed line shows the fit which was obtained with the same assumptions but changing the effective temperature of the star to 6000 K. As one can immediately see in the IR range of the spectrum the quality of the fits are very similar. However, in the optical and ultraviolet (UV) part of the spectrum the fit assuming $T_{\rm eff}$ = 6000 K is not able to explain extinction corrected data. In consequence, we are quite convinced that our estimation of $T_{\rm eff}$ for IRAS 04296 close to 6500 K is reasonable and, what is even more important, agrees pretty well with the spectroscopic estimation (6300 K). Note that spectral type of this source was found to be G0 Ia from the low resolution spectrum (Hrivnak 1995) which implies an effective temperature of around 5500 K for the star if we assume that the same relationship applies for post–AGB supergiants as for "normal" ones (see Schmidt–Kaler 1982). For such a low temperature we were not able to fit even the reddenned data in the UV.

The thin solid line in the wavelength range from about 18 to 48 μm represents the model continuum level found after solution of radiative transfer equation for dust without EOF using the parameters as in Table 2 while keeping the dust temperature (or probability distribution of dust temperature) the same as for the case of dust with EOF. Taking into account the estimated continuum level and assuming that 21 μm feature extends from 18 to 22 μm we estimate the energy emitted in 21 μm band as about 5.7% of the total IR flux (251 $L_\odot$ for λ's from 5 to 300 μm assuming a distance to the source of 1 kpc). With the dotted line for wavelengths longer than 18 μm we present the fit which was obtained using an opacity function with the EOF for only 21 μm component. It is clear that such fit is not able to explain IRAS photometry at 25 μm. Our recent *ISO* observations show that this source is also a 30 μm emitter. In the forthcoming paper (Szczerba et al. 1999) we will discuss this finding in detail.

5. Discussion

As it is shown in Table 1, the metallicity for IRAS 04296 is significantly decreased relative to the solar value: the average abundance for the elements of the iron-group with respect to the Sun is $[(\mathrm{Ti, V, Cr, Fe})/\mathrm{H}]_\odot = -0.9$ with the standard deviation $\sigma = 0.2$.

Recently Decin et al. (1998), using high resolution spectra and model atmospheres method, calculated abundances of 14 chemical elements in the IRAS 04296 atmosphere. Their results are in qualitative agreement with these ones presented here, but there are some significant differences. Decin et al. (1998) calculated the chemical composition of this object assuming $\mathrm{T_{eff}}$ = 7000 K, log g = 1.0, ξ_t = 4 km/s, rather different from the model atmospheres parameters found in this work. It should be noted that we estimated the effective temperature by two independent methods, and it is worth stressing that we have obtained consistent values of the effective temperature: $\mathrm{T_{eff}}$ = 6300 K from numerous Fe I, Fe II spectral lines and $\mathrm{T_{eff}}$ = 6500 K from modelling of the spectral energy distribution of this source. The difference in effective temperature between Decin et al. (1998) and our estimation ($\Delta\,\mathrm{T_{eff}}$ = 700 K) is able to explain different metallicities estimated by Decin et al. (1998) and by us ($\Delta \log \epsilon(\mathrm{Fe}) \approx 0.2$). The same is true for the case of the rare-earth element abundances: large differences, about 1 dex, in the values could be explained by differences in model atmosphere parameters.

Let us consider now in more detail the peculiarities in the chemical composition of the object. For this purpose, in Table 3 we present the logarithmic differences

$$[\mathrm{X/Fe}]_\odot = [\log \epsilon(\mathrm{X}) - \log \epsilon(\mathrm{Fe})]_\star - [\log \epsilon(\mathrm{X}) - \log \epsilon(\mathrm{Fe})]_\odot$$

between chemical compositions of different objects and the Sun (solar abundaces from Grevesse et al. (1996)): in the second column for IRAS 04296, in the third column for IRAS 07134+1005 (hereafter IRAS 07134 – asscociated with the peculiar F–type supergiant HD 56126) and in the fourth one for the star ROA 24. The objects are similar from the point of view of their atmospheric parameters ($\mathrm{T_{eff}}$, log g) and relative chemical composition. It should be noted that the metal deficient supergiant ROA 24 (Fehrenbach's star) belongs to the globular cluster $\omega\,\mathrm{Cen}$ and could be considered as a typical *halo* object in the post-AGB evolution stage.

The carbon overabundance $[\mathrm{C/Fe}]_\odot = +0.8$ (revealed from intensities of 21 absorption lines with the standard deviation $\sigma = 0.46$) and the enhancement of nitrogen $[\mathrm{N/Fe}]_\odot = +0.8$ (from 4 lines, $\sigma = 0.10$) suggest that IRAS 04296 underwent the third dredge–up episode.

The oxygen content based on intensity of 3 weak lines near $\lambda \approx 6155$ Å is determined with a small internal error.

From the Fe–deficiency and CNO abundances ($\mathrm{C/O} > 2$) we can conclude that IRAS 04296 is a low mass object in advanced stage of evolution. For an *unevolved* metal–deficient object (with $[\mathrm{Fe/H}]_\odot \approx -0.9$) the average value of $[\mathrm{C/Fe}]_\odot$ is only about -0.2 (Tomkin et al. 1995), the average value of $[\mathrm{N/Fe}]_\odot$ is ≈ 0 (Wheeler et al. 1989, Timmes et al. 1995) and the average value of $[\mathrm{O/Fe}]_\odot$ is $\approx +0.5$ (Wheeler et al. 1989, Timmes et al. 1995, Klochkova & Panchuk 1996b). The atmospheres of the post-AGB stars IRAS 07134 and ROA 24 are also overabundant in both carbon and nitrogen. Note however, that for most of the PPNe candidates studied, strong relative changes between elements of the CNO–group are observed (Luck et al. 1983; Lambert et al. 1988; Klochkova 1995; Začs et al. 1995, 1996; van Winckel et al. 1996a, 1996b; van Winckel 1997).

The abundances of some light metals (Na, Al, Mg, Si, Ca) are enhanced for all three stars. The average value for these elements is $[\mathrm{X/Fe}]_\odot = +0.6$ for IRAS 04296; +0.9 for IRAS 07134 and +0.6 for ROA 24, with the standard deviations: $\sigma = 0.4$, 0.4 and 0.36, respectively.

We did not still include the K I abundance into our results, since we suspect that the equivalent width of its line near λ 7699 Å could be significantly distorted due to circumstellar and interstellar components.

The iron–group element zinc is the most important for determination of real (initial) value of the metallicity of a star since, firstly, its abundance follows that of iron in a wide $[\mathrm{Fe/H}]_\odot$

Table 3. Relative abundances of chemical elements for IRAS 04296+3429 in comparison to related PPNe. The data by Grevesse & Noels (1996) are adopted for solar abundances.

	IRAS 04296+3429 $[\mathrm{Fe/H}]_\odot = -0.84$	IRAS 07134+1005[a] -1.00	ROA 24[b] -1.77
Element		$[\mathrm{X/Fe}]_\odot$	
Li I	$\geq +0.23$		
C I	+0.84	+1.08	+0.67
N I	+0.83	+1.03	+1.02
O I	+0.19	+0.63	+1.01
Na I	+0.42	+0.54	+0.71
Mg I		+0.97	+0.31
Mg II	+1.34		+0.09
Al I	+1.03	+1.48	
Si I	+0.58	+0.95	+0.80
Si II	+0.26		+1.03
S I	+0.43	+0.63	
Ca I	+0.19	+0.45	+0.60
Sc II	+0.18	-0.07	-0.13
Ti II	-0.27		+0.33
V II	+0.10	-0.03	+0.15
Cr II	+0.11		+0.65
Cu I	+0.24	+1.03	-0.01
Zn I	+0.08		
Y II	+1.20	+1.70	+0.37
Zr II	+0.62		
Ba II	+2.49	+0.99	+0.96
La II	+1.17	+1.59	+0.54
Ce II	+0.82		+1.60
Pr II	+0.74		
Nd II	+1.07	+1.30	+0.67
Eu II	+0.34	+1.06	+0.25

[a] Klochkova (1995),
[b] Gonzalez & Wallerstein (1992).

interval (Sneden & Crocker 1988; Wheeler et al. 1989, Sneden et al. 1991) and, secondly, zinc having a low condensation temperature is not depleted by selective separation processes onto dust grains (Bond 1992). A close to solar abundance of Zn relative to iron ($[\mathrm{Zn/Fe}]_\odot = +0.1$) permits us to conclude about the inefficiency of the selective separation processes in the IRAS 04296 envelope. This conclusion is based also on the absence of overdeficiency of light depleted elements (Ca, Sc). Besides, the relative abundance ($[\mathrm{S/Fe}]_\odot = +0.4$ with the standard deviation $\sigma = 0.21$) of S, a chemical element which is not depleted by dust–gas separation, for IRAS 04296 is close to the value for unevolved metal-deficient dwarfs (François 1987, Timmes et al. 1995). This futher confirms the lack of selective separation in the envelope of the object studied.

Individual abundances of the heavy s-process metals Y and Zr are determined with a relatively large error because of the small number of lines measured. However, the average value $[\mathrm{X/Fe}]_\odot = +0.9$ for Y and Zr is sufficiently reliable. In addition, the abundance of heavy s-process element Ba ($[\mathrm{Ba/H}]_\odot = +2.5$) derived from the equivalent width of strong lines could be altered by a systematic error due to the complexity of the outer regions of the stellar atmopshere as discussed above. Nevertheless, we conclude that there is a Ba excess.

The abundance of lanthanides (La, Ce, Pr, Nd) are strongly enhanced relative to iron for the objects from Table 3. For these heavy metals the average value is $[\mathrm{X/Fe}]_\odot = +1.0, +1.4, +0.9$ for IRAS 04296, IRAS 07134 and ROA 24, respectively, with the standard deviations 0.2 and 0.6 for IRAS 04296 and ROA 24. Moreover, for all these objects we see the overabundance of Eu which is predominantly produced by the r–process.

Excess of s-process elements has been reliably found up to now in three objects investigated at the 6 m telescope: IRAS 04296+3429, IRAS 07134+1005 and IRAS 22272+5435. Besides, similar conclusions have appeared for another four PPN candidates (and for one object in common): HD 158616 (van Winckel et al. 1995); IRAS 19500-1709 = HD 187885 (van Winckel 1997); IRAS 05341+0852 (Reddy et al. 1997); IRAS 22223+4327 and IRAS 04296+3429 (Decin et al. 1998). In atmospheres of most PPN candidates overdeficiency (with respect to their metallicity) of heavy nuclei is generally observed (Klochkova 1995; van Winckel et al. 1996a, 1996b; Klochkova & Panchuk 1996a; van Winckel 1997), whose existence in the atmospheres of post–AGB low–mass supergiants has not yet found a clear explanation.

In consequence, we can state that the chemical abundances pattern for the source IRAS 04296 is related to its old galactic population membership and dredge–up of matter enriched by the nucleosynthesis products. It may be part of the old disk population.

As has been concluded already by Decin et al. (1998) all the post–AGB candidates mentioned above (only these, up to now, show an s–process element enhancement!) belong to the small group of PPNe (Kwok et al. 1989; Kwok et al. 1995) which have in their IR spectrum an unidentified emission band at about 21 μm. This feature is neither found in the spectra of their predecessors, AGB stars, nor in the spectra of PNe. Note, once more, that the search by means of the *ISO* for the new 21 μm emitters among candidates selected by Henning et al. (1996) failed (Henning, private communication). As has been stated in the papers by Kwok et al. (1989, 1995), the objects whose spectra contain the 21 μm band are carbon-rich stars. Our investigations based on the spectra from the 6 m telescope, for IRAS 07134 (Klochkova 1995), IRAS 22272+5435 (Začs et al. 1995) and IRAS 04296 (Klochkova et al. 1997b), confirmed that $\mathrm{C/O} > 1$ for all of them. In this context, the conclusion that the carrier of the 21 μm band is related to C is natural. For example, Buss et al. (1990) have supposed that this feature may be caused by polycyclic aromatic hydrocarbons. On the other hand, Goebel (1993) has identified the 21 μm band with the vibrational band of the SiS_2 molecule, the presence of which is consistent with the temperature in the envelope.

Taking into account the available results on chemical composition for subclass of PPNe with the 21 μm feature: IRAS 07134+1005 (Parthasarathy et al. 1992, Klochkova 1995), IRAS 22272+5435 (Začs et al. 1995), IRAS 19500-1709 (van Winckel et al. 1996a), IRAS 05341+0852 (Reddy et al. 1997), IRAS 22223+4327 (Decin et al. 1998), and IRAS 04296 (Decin et al. 1998; Klochkova et al. 1997b; this paper) we see that the carbon-rich atmospheres of these objects are also enriched by s–process elements. It is evident that there is a strong correlation between the presence of the 21 μm feature, C_2, C_3 molecular bands, and the excess of the s–process elements. Decin et al. (1998) were the first who pointed out this relationship. What is even more important, an excess of s–process elements was not found for a number of IRAS sources with altered CNO-content but without the 21 μm feature (some of which are oxygen-rich stars rather than carbon-rich stars): IRAS 06338+5333 (Luck & Bond 1984; Bond & Luck 1987), IRAS 07331+0021 (Luck & Bond 1989; Klochkova & Panchuk 1996a), IRAS 09276+4454 (Klochkova & Mishenina 1998), IRAS 12175−5338 (van Winckel 1997), IRAS 12538−2611 (Luck et al. 1983; Klochkova & Panchuk 1988b; Giridhar et al. 1997), IRAS 15039−4806 (van Winckel et al. 1996b), IRAS 17436+5003 (Klochkova & Panchuk 1988a; Luck et al. 1990; Klochkova 1998), IRAS 18095+2704 (Klochkova 1995), and IRAS 19114+0002 (Začs et al. 1996, Klochkova 1998). Therefore, it seems that carrier of 21 μm feature is *strongly* related to the whole chemical composition pattern typical for the third dredge–up (excess of s-process elements), and not only to the C-richness of the photosphere.

That 21 μm feature is not observed around AGB–stars showing s–process elements could be explained by the physical conditions which are inappropriate for the excitation of this band, while its non–presence in planetary nebulae may be a result of carrier destruction by the highly energetic photons.

6. Conclusions

We conlude that IRAS 04296+3429 is a PPN candidate with a chemical composition which coincides with theoretical predictions for the post–AGB objects: very large excesses of carbon

and nitrogen are revealed. Moreover, the real excess (relative to iron) of heavy metals Y, Zr, Ba, La, Ce, Pr, Nd synthesized by the neutronization process indicates an effective third dredge–up and further confirms IRAS 04296 to be in the advanced post-AGB evolution stage.

The emission of C_2 molecular lines discovered in the spectra of IRAS 04296 and its similarity to the emission of the Hale–Bopp comet allow us to suggest that in both cases the same mechanism (the resonance fluorescence) is responsible for the observed features.

Several strong absorptional features whose positions coincide with known diffuse interstellar bands (DIBs) are found in the spectrum of IRAS 04296.

In addition, from the SED modelling of the spectral energy distribution we showed that 25 μm flux cannont be explained without assumption that the 30 μm emission feature is present in this source. Our recent *ISO* observation has detected the 30 μm band in this source.

Acknowledgements. We are much indebted to the referee Hans van Winckel for his critical reading of the manuscript and valuable advice. This work has been supported by project 1.4.1.1 of the Russian Federal Program "Astronomy" and grant 2.P03D.002.13 of the Polish State Committee for Scientific Research. One of us (R.Sz.) gratefully acknowledges the support from the Canadian Institute of Theoretical Astrophysics.

References

Bakker E.J., van Dishoeck E.F., Waters L.B.F.M., Schoenmaker T., 1997, A&A 323, 469
Boesgaard A.M., 1989, ApJ 336, 798
Bond H.E., 1992, Nat 356, 474
Bond H.E., Luck R.E., 1987, ApJ 312, 203
Burstein D., Heiles C., 1982, AJ 87, 1165
Buss R.H., Cohen M., Tielens A.G.G.M., et al., 1990, ApJ 365, L23
Cardelli J.A., Clayton G.C., Mathis J.S., 1989, ApJ 345, 245
Crampton D., Cowley A.P., Humphreys R.M., 1975, ApJ 198, L135
Decin L., van Winckel H., Waelkens C., Bakker E.J., 1998, A&A 332, 928
François P., 1987, A&A 176, 294
Giridhar S., Rao N.K., Lambert D., 1994, ApJ 437, 476
Giridhar S., Ferro A.A., Paraao L., 1997, PASP 109, 1077
Goebel J.H., 1993, A&A 278, 226
Golden S.A., 1967, JQSRT 7, 225
Gonzalez G., Wallerstein G., 1992, MNRAS 254, 343
Grevesse N., Noels A., Sauval A.J., 1996, ASP Conf. Ser. vol. 99, p. 117
Gustafsson B., Bell R.A., Eriksson K., Nordlund A., 1975, A&AS 42, 407
Henning Th., Chan S.J., Assendorp R., 1996, A&A 312, 511
Hrivnak B.J., 1995, ApJ 438, 341
Hrivnak B.J., Kwok S., Geballe T.R., 1994, ApJ 420, 783
Iyengar K.V.K., Parthasarathy M., 1997, A&AS 121, 45
Jenniskens P., Ehrenfreund P., Foing B., 1994, A&A 281, 517
Klochkova V.G., 1995, MNRAS 272, 710
Klochkova V.G., 1998, Bull. SAO 44, 5
Klochkova V.G., Mishenina T.V., 1998, Bull. SAO 44, 83
Klochkova V.G., Panchuk V.E., 1985, Bull. SAO 20, 12
Klochkova V.G., Panchuk V.E., 1988a, SvA Let 14, 77
Klochkova V.G., Panchuk V.E., 1988b, SvA Let 14, 933
Klochkova V.G., Panchuk V.E., 1996a, Bull. SAO 41, 5
Klochkova V.G., Panchuk V.E., 1996b, Astronomy Reports 40, 829
Klochkova V.G., Panchuk V.E., 1998, Pis'ma Astron. Zhurn 24, 754
Klochkova V.G., Chentsov E.L., Panchuk V.E., 1997a, MNRAS 292, 16
Klochkova V.G., Panchuk V.E., Szczerba R., 1997b, In: Waters L.B.F.M., Waelkens C., van der Hucht K.A., Zaal P.A.(eds.) ISO's view on stellar evolution. Ap&SS 255, 485
Krishna Swamy K.S., O'Dell C.R., 1977, ApJ 216, 158
Krishna Swamy K.S., O'Dell C.R., 1979, ApJ 231, 624
Krishna Swamy K.S., O'Dell C.R., 1981, ApJ 251, 805
Kurucz R.L., 1979, ApJS 40, 1
Kwok S., 1993, ARA&A 31, 63
Kwok S., Hrivnak B.J., Geballe T.R., 1995, ApJ 454, 394
Kwok S., Volk K., Hrivnak B.J., 1989, ApJ 345, L51
Lambert D.L., Hinkle K.H., Luck R.E., 1988, ApJ 333, 917
Loup C., Forveille T., Omont A., Paul J.F., 1993, A&AS 99, 291
Luck R.E., 1991, ApJS 75, 759
Luck R.E., Bond H.E., 1984, ApJ 279, 729
Luck R.E., Bond H.E., 1989, ApJ 342, 476
Luck R.E., Bond H.E., Lambert D., 1990, ApJ 357, 188
Luck R.E., Lambert D.L., Bond H.E, 1983, PASP 95, 413
Omont A., Loup C., Forveille T., Te Lintel Hekkert P., 1993, A&A 267, 515
Omont A., Mosley S.H., Cox P., et al., 1995, ApJ 454, 819
Panchuk V.E., Najdenov I.D., Klochkova V.G., et al., 1998, Bull. SAO 44, 127
Parthasarathy M., Garcia-Lario P., Pottash S.R., 1992, A&A 264, 159
Reddy B.E., Parthasarathy M., Gonzalez G., Bakker E.J., 1997, A&A 328, 331
Rouleau F., Martin P.G., 1991, ApJ 377, 526
Schmidt-Kaler Th., 1982, Physical parameters of the stars. In: Schaifers K., Voigt M.H. (eds.) Landolt Börnstein A&A Vol. VI, 2b. Springer, Berlin, p. 451
Sneden C., Crocker D.A., 1988, ApJ 335, 406
Sneden C., Gratton R.G., Crocker D.A., 1991, A&A 246, 354
Swings P., 1941, Lick Observ. Bull. 19, 31
Szczerba R., Volk K., Kwok S., 1996, In: Käufl H.U, Siebenmorgen R. (eds.) ESO Workshop, The role of dust in formation of stars. p. 95
Szczerba R., Omont A., Volk K., Cox P., Kwok S., 1997, A&A 317, 859
Szczerba R., Henning Th., Volk K., Kwok S., Cox P., 1999, A&A submitted
Timmes F.X., Woosley S.E., Weaver T.A., 1995, ApJS 98, 617
Tomkin J., Woolf V.M., Lambert D., Lemke M., 1995, AJ 109, 2204
Tsymbal V., 1995, In: Adelman S.J., Kupka F., Weiss W.W (eds.) Model Atmospheres and Spectrum Synthesis. ASP Conf. Ser. vol. 108, p. 198
van Winckel H., 1997, A&A 319, 561
van Winckel H., Mathis J., Waelkens C., 1992, Nat 356, 500
van Winckel H., Waelkens C., Waters L.B.F.M., 1995, A&A 293, L25
van Winckel H., Waelkens C., Waters L.B.F.M., 1996a, A&A 306, L37
van Winckel H., Oudmaijer R., Trams N.R., 1996b, A&A 312, 553
Waelkens C., van Winckel H., Bogaert E., Trams N.R., 1991, A&A 251, 495
Wheeler J.C., Sneden C., Truran J.W.Jr., 1989, ARA&A 27, 279
Zanstra H., 1928, MNRAS 89, 178
Začs L., Klochkova V.G., Panchuk V.E., 1995, MNRAS 275, 764
Začs L., Klochkova V.G., Panchuk V.E., Spēlmanis R., 1996, MNRAS 282, 1171